CONFIGURATION OF MAGNETIC FIELDS IN A QUIET PHOTOSPHERE AS REVEALED BY COMPARING THE VALUES OF THE LONGITUDINAL FIELD MEASURED BY THE COG METHOD FOR TWO LINES

© 2025 S. G. Mozharovsky (https://orcid.org/0000-0002-5552-8254)

Institute of Applied Astronomy RAS, Saint Petersburg, Russia

e-mail: mozharovskys@mail.ru

Received February 24, 2025

Revised April 21, 2025

Accepted June 17, 2025

Abstract. The estimate of the longitudinal magnetic field obtained from the Hinode spectropolarimeter data will be different if it is determined in different ways. In particular, the values obtained by the Centers Of Gravity (COG) method for the Fe I λ 6301 and 6302 Å lines do not coincide. Some of the differences are due to the different inaccuracies of the COG method for each of the two lines. However, some of the differences can be explained by the fact that the response functions of these lines to changes in the magnetic field are formed at different heights. This should be accompanied by a certain morphological picture of magnetic fields. It consists in the fact that most of the magnetic configurations of the quiet photosphere are similar to each other. To a rough approximation, their structure can be compared with the structure of a sunspot – there is a central region with the strongest field, close to vertical, and slopes – an analog of penumbra, where the field weakens and / or turns to horizontal. This turn occurs at the heights of the greatest response of the Fe I λ 6301 and 6302 Å lines to changes in the magnetic field with a reversal length of about tens of kilometers.

Keywords: *Hinode SOT/SP, longitudinal magnetic fields, Quiet Sun, COG method*

DOI: 10.31857/S00167940250712e8

1. INTRODUCTION

There is a problem of differences in the magnetic field data that are obtained when the field is measured using different methods. It is convenient to represent such differences graphically (see Fig. 1), taking advantage of the extensive data that the Hinode spectropolarimeter collects. First, there are differences between the values of the longitudinal field in the quiet photosphere measured by the inversion method from the Milne-Eddington model (ME-inversion), denoted as $B_{\mathrm{ME},\|}$, and by the method of Stokes I+ V and I-V (Center Of Gravity - COG) profiles, denoted as B_{IV}, see Figures 1 (a) and (b) for the quiet photosphere, (d) and (e) for the penumbra. The differences between $B_{(\mathrm{ME})_{(,\|)}}$ and B_{IV} are not large, some of them can be explained by errors in the COG technique (see Section

3). Obviously, the response functions, in particular the effective response depths for the COG and ME-inversion methods, are different. However, this difference is due to such a large number of factors that it is not yet possible to analyze it and relate it to physical conditions in the photosphere. Another case is the difference in the longitudinal field magnitudes measured by the COG method separately for the Fe I λ 6301 and 6302 Å lines. While for the penumbra (Fig. 1(f)) the differences are minimal and are due to the difference in the application of the COG method to the different lines, in the case of the quiet photosphere (Fig. 1(c)) the difference at first sight requires a sharp increase of the longitudinal field with height. A second option to explain the picture in Figure 1(c), is to involve a Filling Factor (*f*) model in which the magnetic field occupies only part of the area. The required ratio of measured values can be explained by the difference of Stokes *I* profiles in magnetic and non-magnetic elements [Domínguez Cerdena et al. 2003, Botygina et al. 2017].

In Fig. 1, the upper and lower rows show data for two observing sessions. In the top row is a typical session with a quiet Sun of the largest possible size for SP Hinode. In the bottom row is one of the sessions where a significant part of the area is occupied by the penumbra of a complex group of spots.

If the measurement methods had no errors, their results would be the same. The differences indicate either possible errors in the methods or that we are getting data from different volumes of matter. For example, from volumes lying at different altitudes. Or on different parts of the aperture area, when the source of the Stokes *V*-profile is located inside the area with magnetic field, and the source of the I-profile is located on the whole area. So, according to Figures 1 (a and b), in the quiet photosphere the flux ratios $k_{MEIV} = f \cdot B_{ME,\|}/B_{IV}$ vary from 0.7 at B_{IV} = 30 Mx cm^{-2} to 1.5 at B_{IV}= 350 Mx cm^{-2}. In the penumbra (Figures 1 (d, e)) k_{MEIV} reach 0.8 and 1.2 at B_{IV} = 60 and 1100 Mx cm^{-2}, respectively. More interesting are the longitudinal field differences made by the same method for two different lines. While in the penumbra (Fig. 1 (f)) the differences are insignificant, the values of $k_{12} = B_{IV,6301}/B_{IV,6302}$ differ from unity by less than 5%, and can be written off as a difference in the accuracy of the method for these lines, according to Fig. 1 (c) the value of $k_{(12)}$ in the quiet photosphere reaches on average 1.3 for B_{IV}50-80 Mx cm^{-2} ($\log_{10}(k_{12}) \approx 0.12$). The value k_{12}= 1.3 was obtained in other works using SP/Hinode data [Botygina et al., 2017]. In [Domínguez Cerdena et al., 2003], k_{12}= 1.25 ± 0.14.

2. DATA

This work is based on data acquired by the SP spectropolarimeter [Lites et al., 2013] of the SOT solar optical telescope [Tsuneta et al., 2008] of the Hinode satellite mission [Kosugi et al., 2007]. Level 1 data that have already undergone preprocessing are used. The main material analyzed is the quiet photosphere without division into grid regions (Network, NW) and regions inside supergranules (InterNetwork, IN). In the present work, the quiescent photosphere is

represented by an observing session that we identify as 20070310_1137 (see Fig. 2(a)). The first eight digits denote the date in the format YYYYYYYMMDD, the last four digits denote the hours and minutes of the session start time. This session is one of the most studied sessions from the work of [Lites et al., 2008] to [Amari et al., 2024]. As illustrations, the centroid of this session's 40×40 angular second map (also as done in [Lites et al., 2008]) will be shown below. It is convenient to use session 20141024_0031 (Figure 2(b and c)) to analyze the penumbra.

The SP/Hinode data are intensities in Stokes parameters I, Q, U, V recorded for 112 points in the spectrum in the wavelength range 6300.9-6303.0 Å in steps of about 21.6 mÅ. The polarimeter can record up to 1024 points along the slit in 0.16" steps, also the slit can be moved along the surface up to 2047 steps in 0.15" steps. The SOT telescope limits the angular resolution to a value of 0.32", which is related to its diffraction limit. In this paper, maps recorded with an exposure of 4.8 s for each slit position are used.

In the case of studying the magnetic field of the quiet photosphere, it is necessary to preliminarily discard, filter out the map points that do not contain the magnetic field. We will assume that these are the points for which the values of the Stokes parameters Q, U, and V in the sum are less than some threshold value. We define the polarization value as $P = \sqrt{(Q^2 + U^2 + V^2)}$, where the values of Q, U, and V are divided by the continuum level of the continuous spectrum I_C. By summing the values of P along the line profiles, the equivalent polarization width $W_{(P)}$ can be determined by analogy with the equivalent line width $W_I = \int_{\lambda_1}^{\lambda_2} \frac{I}{I_C} d\lambda$. The value of W_P can be described as the area of the figure under the polarization curve. It has the dimension of wavelength, as does the X-axis of the figure, since the Y-axis is dimensionless. We determine the values of λ_1 and λ_2 by one of two criteria - either the intensity in the wing profile $I(\lambda)$ becomes less than 95% of I_C, or the distance from the center of the line λ_0 exceeds 300 mÅ. A histogram was constructed for the W_P values of all 2-10^6 map points. Assuming that most points of the quiet photosphere do not contain a magnetic field, the position of the top of the histogram gives us the average value of the noise level. It is 1.6 mÅ. When plotting the scatter diagrams, we will limit ourselves to the value W_P= 3.3 mÅ, thus discarding 92.5% of the map points for session 20070310_1137.

The W_P values are important for estimating the polarization in the lines. However, the value of P_{tot}, which was used by [Lites et al., 2008], turns out to be more convenient for determining the noise level. Our method is identical to that of these authors, the difference being a constant factor, $P_{tot} = W_P/1200$. The cutoff bound P_{tot}= 0.004 adopted in their work corresponds to W_P= 4.8 mÅ. The point is that the authors of this paper divided the integral by the length of the integrand. The values of λ_1 and λ_2 they chose are -300 to +300 mÅ for each of the two lines, totaling (300+300)-2=1200.

The data for the COG method are obtained by simply summarizing the Stokes *I* and *V* profiles using formula (2) from Section 3. The flux f-$B_{ME,\|}$ is obtained by multiplying three physical parameters that can be found in the Level 2 (Level 2) FITS files, namely field strength $|B|$ = Field_Strength, the cosine of the angle of inclination of the lines of force to the beam of view cos(γ), where γ = Field_Inclination, and the fill factor f = Stray_Light_Fill_Factor.

3. METHOD OF CENTERS OF GRAVITY

The method of centers of gravity is voiced in [Semel, 1967] as well as [Rees & Semel, 1979]. It is based on the fact that the difference in the positions of the centers of gravity (Center Of Gravity - COG) of the I+ V and I-V Stokes profiles is equal to the magnitude of the magnetic splitting of the spectral line according to the formula (here the values of λ are given in cm):

$$(\lambda_{I+V} - \lambda_{I-V}) / 2 = 4.6686 \cdot 10^{-5} \cdot \lambda^2 \cdot g_{eff} \cdot B_{\|} , \quad (1)$$

The wavelengths of the centers of gravity $\lambda_{I \pm V}$, where $I_{I \pm V} = I_C - (I \pm V)$, are calculated as sums:

$$\lambda_{I \pm V} = \Sigma(I_{I \pm V} \cdot \lambda \cdot \Delta\lambda) / \Sigma(I_{I \pm V} \cdot \Delta\lambda), \quad (2)$$

$B_{\|}$ of (1) is the longitudinal component of the magnetic field calculated by the COG method, as synonyms throughout the text we use the notation $B_{I \pm V}$, or simply B_{IV}.Also $B_{\|}$ = | B|-cos(γ), where γ is the angle between the magnetic field vector and the beam of view.

Formulas (1) and (2) can be written in an alternative formulation. In this case, the method is called the method of moments of the Stokes *V-parameter* [Mathys, 1988]. More precisely, it is the first moment of the Stokes *V-parameter* normalized to the equivalent spectral line width:

$$M_V = \frac{\int_{\lambda_1}^{\lambda_2} (\lambda - \lambda_0) \cdot V \cdot d\lambda}{W_I} \quad (3)$$

The moment $M_V$in formula (3) coincides in meaning with the difference of positions of the centers of gravity $\lambda_{I \pm V}$from formula (2). The results of field calculation by formulas (2) and (3) coincide. The form of the record (3) allows us to understand that when the Filling Factor (f) is small, i.e., when the fraction of area in the spectrograph aperture that is occupied by regions with magnetic field is small, the result can be distorted. Namely, the surface areas that are responsible for the formation of the Stokes profiles $V(\lambda)$ and $I(\lambda)$ may not coincide. This will distort the values of $M_V$for the Fe I λ 6301 and 6302 Å lines to different degrees.

Thus, the presence of thin kiloGaussian tubes can change the described ratio of the fluxes of the extended field k_{12}. Schematically, the distortion mechanism can be described as follows. It is known that the line profiles weaken in regions of the photosphere with magnetic field outside the spots. Let the field B_0=1000 Gs, the fraction of the area with the field f=*0.*1 and the equivalent line width Fe I λ 6302 Å decreases by a factor of two r_2=0.5, where r is the coefficient of change of the equivalent line width in the magnetic field with respect to the nonmagnetic photosphere. Then the measured flux will be $B_{IV,6302}$=$B_0 f r_2$= 50 Gs. If $W_{(I),6301}$decreases in the magnetic field by a factor

of 1.5, $r_1 \approx 0.7$, then $B_{IV,6301}$ will be 70 Gs. Total, the ratio of measured longitudinal field strengths $k_{12}=1.4$. Obviously, the values of $B_0$and f for both lines are the same, hence it follows that k_{12}can be calculated simply as r_1/r_2. In the paragraph above, the specific values of $r_{(1)}$and $r_2$were taken only for clarity. We can use the specific observed values of $W_I$for session map 20070310_1137 for two statistical subsets of points. One subset is the map points without field filtered by $W_P < 3$mÅ, The second subset is points with values B_{ME} = Field Strength > 900 Gs and filling factor $f > 0.75$. The following figures are obtained:

Line / Value	$W_{(I)}$ (without field), mÅ	W_I (B_{ME}>900 G, f>0.75), mÅ	$r=W_{I,B>900}/W_{I,B=0}$
6301	126.5	97.4	0.694
6302	87.8	65.0	0.667

Whence $k_{12}\sim1.05$. It follows that either the kilohauss thin tubes cannot provide the mean observed value of $k_{12}=1.3$. Or the photospheric model for these tubes must be very different from the photospheric model of homogeneous regions with magnetic field ($f=1$).

The method of centers of gravity, equivalent to the normalized V-parameter momentum method Stokes, has important useful properties. The difference in the positions of the centers of gravity $\lambda_{\pm}$ is linearly related to the strength of the longitudinal component of the magnetic field. The linearity has important implications:

1. The result of the calculation will not change if the photospheric model is changed
2. It should work equally well for any magnetically active line.

That is, when making measurements in the shadow, penumbra, and calm photosphere regions we should get uniform correct results. We will also get the same results when making measurements in different spectral lines, in particular in the Fe I λ 6302 and 6301 Å lines.

It is also important that when integrating formula (3) the distortions of V values caused by noise are averaged.

In the course of this work, a number of calculations of Stokes profiles for a one-dimensional model of the photosphere were performed, in particular, the HOLMU model was used [Holweger & Muller 1974]. The calculation program [Mozharovsky 2013] is a functional analog of the MALIP [Landi Degl'Innocenti 1976] and SPANSAT [Gadun & Sheminova 1988] codes. The computations revealed the following important properties:

1. The result is independent of the convolution of the Stokes profiles with the spectrograph hardware function or with the Doppler broadening of macro- and microturbulent velocities. Moreover, even extremely large linear gradients of the radial velocity have no appreciable effect on the result as long as the field strength is constant with height.

2. Also, the result depends little on the wavelength step of the profiles, i.e. for measurements with steps of, for example, 10, 20, and 30 mÅ, the calculation results will be approximately the

same.

In calculations for weak lines (equivalent widths W_I< 15 mÅ in the red region), the validity of formula (1) is preserved to within a few percent. The values of B_{IV}decrease for strong lines, i.e., lines with larger equivalent widths.

The properties of the COG method for the Fe I λ 6302 and 6301 Å lines obtained by numerical calculations for the one-dimensional photospheric model are shown in the graphs (Figure 3).

As these calculations show, the COG method generally underestimates the field values. The underestimation depends on the angle of the field to the beam of view γ, on the field strength, and on the line. In particular, at $\gamma=0°$ *the* COG method works without distortion, but it is clear that real fields are rarely directed exactly toward the observer. For the Fe I λ 6301 Å line, the B_{IV}values are systematically smaller than for Fe I λ 6302, although only by a couple of percent, but the k_{12}values can also reach 0.8 - 0.9 at strengths larger than 10^3Gauss. This can in no way explain the observed average difference in the quiet photospheric strengths k_{12}= 1.3 (see Figure 1(c)). And here are the differences between the field values in the penumbra obtained by the ME-inversion and the COG method (Figure 1(e)) k_{MEIV}= 1.1 - 1.2 can be explained by the underestimation by the COG method alone.

Separately, we note that the data obtained by the COG method for the spot shadow - i.e., for regions with a continuous spectrum level $I_C < 0.3\ I_{QS}$ (QS – Quite Sun) - are unreliable due to the large number of molecular (and not only) blending lines. These lines themselves have polarization in the magnetic field, and also do not allow to determine the level of the continuous spectrum, and thus to calculate the equivalent width W_I, which is included in the formulas for calculating B_{IV}.

4. THE RATIO OF $B_{IV,6301}/B_{IV,6302}$ AND THE THE DIFFERENCE OF THE RESPONSE HEIGHTS FOR THE TWO LINES

As stated in the introduction according to Figure 1(c) the longitudinal field measured in the Fe I λ 6301 Å line in the quiet photosphere exceeds the field measured in the Fe I λ 6302 Å line on average by 30% (k_{12}= 1.3) for B_{IV}50-80 Mx cm^{-2}and decreases to k_{12}= 1.15 for strengths of 350 Mx cm^{-2}. One possible explanation is that the longitudinal field varies with height, and the response functions for COG measurements for different lines have different effective heights. The widespread increase of the field with height in the magnetic elements of the quiescent photosphere contradicts the known concepts. Therefore, it is necessary to find such conditions under which the response height for the Fe I λ 6301 Å line is deeper than for Fe I λ 6302 Å.

In order to analyze the response heights, a series of calculations of the effective response heights of the value $B_{I\pm V}$to changes in the magnetic field strength B were performed. The calculation was done by numerical method. In this method, a series of calculations is carried out

with different heights of some "trial" layer, where a certain physical parameter is given a special increment on the height interval Δh, for example, $B = B_0$+10 Gs. For the value $B_{I\pm V}$ calculated from formula (2) we find variations, i.e. the response function (Response Function - RF $B_{I\pm V}$), and plot it on the graph RF(h). We take the position of the center of gravity of the response function as the effective response height. As calculations have shown, the appearance of RF functions practically does not depend on the field strength (at photospheric values, i.e., $B \leq$ 1000 Gs), and also depends little on the inclination of the field vector to the beam of view γ. There is a dependence on the photospheric model, see Figure 4 (a), (b). But it does not qualitatively change the height ratio for the Fe I λ 6301 and 6302 Å lines. As it turned out, the $B_{I\pm V}$response for the Fe I λ 6301 Å line is born deeper than the response for Fe I λ 6302 Å, but the height difference is very small. Everyone knows that stronger lines are born higher than weaker lines. But this turns out to be incorrect, if we determine a value that requires integration of the whole profile, not just the central part of it. We divided the $I\pm$ V profiles into 9 equal intervals along the residual intensity I/I_C of each line and repeated the calculation of the effective heights, see Fig. 5. The central part of the Fe I λ 6301Å line profile is formed highest of all, as expected. But each individual fragment of the profile with the same residual intensity for line 6301, is formed deeper than for line 6302. Nevertheless, the difference in the response heights of the lines is small. To explain the difference in the measured field strength k_{12}= 1.3, we must assume rather large gradients of the longitudinal field. Why can the longitudinal component of the field change rapidly with height? Probably due to its reversal from the vertical to the horizontal position. We can assume that the abundant [Lites et al., 2008] horizontal fields B_T= 55 Mx cm^2 are entrained by convective motion into the intergranular gaps, where they turn into vertical ones rather quickly. Let us add the following field configuration to the HOLMU photospheric model [Holweger & Muller, 1974] - the absolute value of the field in the B_0 model is constant. The angle of inclination of the field to the line of sight in deep layers is 0°, in high layers it is 90°, and at some interval Δh_t (h_t – Height of Turn), the center of which is at height h_t, varies linearly with height. Let us calculate the profiles and compare the values of $B_{IV,6301}$ and $B_{IV,6302}$. In this simple way we were able to obtain values of k_{12}up to 1.2, see Figure 6(a). However, such values are obtained under some conditions. In both directions from some peak near 900 Gs the value of k_{12}decreases markedly. Decreasing the turning altitude interval increases k_{12}. But even at Δh_t= 40 km, the best value of k_{12} is still close to 1.2. The model also allows us to calculate the limiting (physically unrealistic) case Δh_t= 0, which allows us to consider limiting values (Figures 6 (b and c)). If we change the average turning height (in the range of h_t= 0-100 km above τ_5 = 0), this does not significantly change k_{12}, but very strongly changes the apparent longitudinal field strength. To get the most frequent statistical observed B_{IV} values of ~50-80 Gs the turning altitude for the HOLMU model must fall between 20 and 80 km. If it is higher,

we would get observed longitudinal B_{IV}fields of ~200-300 Gs, while lower ones would be on the order of 10 Gs. This gives rise to the assumption that the optical depth τ_5, at which we see the "reversal", may be changing in the grid region. This gives rise to both the measured strengths B_{IV}~300-800 Gs and the fact that the values of k_{12} fall to 1.

It should be noted that all calculations made above assume a one-component one-dimensional model of the photosphere. That is, the change of the photosphere in the plane is significantly smaller than its changes in the vertical direction. The second remark is that the calculations do not include radial velocities, which, in the presence of altitude gradients, can significantly change the effective response heights in the wings of the lines. Therefore, the obtained figures can be considered as a preliminary conditional estimate. What can be said more definitely, the magnetic structures in the quiescent photosphere are morphologically homogeneous. Any magnetic field hill on the periphery is surrounded by a region in which the longitudinal field is smaller than in the center. As we see in the map in Figure 7(b), these peripheral regions have significant values of $k_{(12)}$ (on average of the order of 1.3), relatively small measured B_{IV} fields of ~50-80 Gs, and significant weight in the statistics. One explanation for the large values of k_{12} is that here we observe a reversal of the lines of force from horizontal to verical direction as the lines of force are pulled into the lower layers of the photosphere by downward convective flows.

5. CONCLUSIONS

The method of COG centers of gravity allows us to expect almost identical values of the longitudinal field measured with the Fe I λ 6301 and 6302 Å lines if the field is uniform in height and within the aperture of the spectrograph. In practice, the ratio of the strengths in these lines everywhere in the quiet photosphere is noticeably greater than unity, on average k_{12}= 1.3. This presents a mystery to researchers, as noted in the review [Bellot Rubio & Orozco Suárez, 2019]. Apparently, the explanation is that these lines reflect the state of the field strength in different volume elements of the photosphere. Traditionally, starting with [Stenflo, 1973], it has been assumed that the quiescent photosphere is permeated by ubiquitous thin force tubes of very small diameter. The presence of these tubes affects the results of all magnetic field measurements in one way or another. In particular, the observed strength ratio k_{12}= 1.3 is also explained by some authors within this approach [Domínguez Cerdena et al., 2003; Botygina et al., 2017]. However, in the framework of the present work, another possibility is proposed. Namely, the influence on the measurement results of field inhomogeneity not in the aperture plane, but along the viewing beam. The paper shows that the commonly accepted notion that a stronger line always brings a response about the physical properties of the medium from higher altitudes is incorrect. In particular, the response to changes in field strength for the Fe I λ 6301 Å line originates deeper than the response of the Fe I λ 6302 Å line. However, the difference in response heights is small, requiring a

sufficiently sharp change in the magnitude of the longitudinal field with height to explain the observed ratio k_{12}= 1.3. As a result of model calculations, it was shown that the observed ratio can be partially explained by assuming a sharp change in the inclination of the magnetic field lines with height from a nearly vertical field in the depth, to a nearly horizontal field in the outer layers. The interval over which the change occurs must be quite narrow - tens of kilometers. The height in the photosphere, at which such a change occurs, also has a certain value, it should be within the range from 0 to 100 km above τ_5= 1, so that the measured longitudinal field B_{IV}turns out to be in the interval of the most probable statistically values 50-80 Mx cm^{-2}. This picture to some extent agrees with the excess of the horizontal field flux found in the regions inside the supergranules (IN - InterNetwork regions) [Lites at al, 2008] the excess of the horizontal field flux of 55 Mx cm^{-2}over the vertical one of 11 Mx cm^{-2}. Also in two papers [Stenflo, 2013] and [Lites at al., 2017] a study of the direction of the polarization plane near the limb was made. From these studies, it follows that at some height the field is predominantly horizontal with respect to the solar surface, but as we move to deeper layers, the field becomes more vertical. Finally, the distribution of the k_{12}magnitude over the Hinode session map for the quiescent photosphere (Figure 7 b) shows its increase around the periphery of the magnetic field hills, which may indicate an abrupt change in the field direction at these locations.

FUNDING

This work was funded from the Institute's budget. No additional grants were received to conduct or supervise this particular study.

CONFLICT OF INTERESTS

The author declares that he has no conflict of interest.

REFERENCES

1. *Gadun A.S., Sheminova,V.A.* SPANSAT: A program for calculating spectral absorption line profiles in stellar atmospheres in the LTR approximation // Preprint ITF1988, Institute of Theoretical Physics of the Academy of Sciences of the Ukrainian SSR: Kiev. P. 37.
2. *Mozharovsky S.G.* Development of the SunWorld software package. An overview of the properties and methods of SunWorld from the 1990 version to the modern one // Solar activity and its influence on the Earth. Yearbook of the UAFO Far Eastern Branch of the Russian Academy of Sciences V. 15. P. 76-110. 2013.
3. *Amari T., Canou, A., Velli, M., et al.* The Ubiquity of Twisted Flux Ropes in the Quiet Sun // DOI: 10.48550/arXiv.2411.10563. 2024.
4. *Bellot Rubio, L., Orozco Suárez, D.* Quiet Sun magnetic fields: an observational view // Living Reviews in Solar Physics V. 16. P. 1. 2019.

5. *Botygina O., Gordovskyy M., Lozitsky V.* Investigation of Spatially Unresolved Magnetic Field Outside Sunspots Using Hinode/SOT Observations // Astroinformatics. M. Brescia V. 325 P. 59-62. 2017.
6. *Domínguez Cerdeña, I., Sánchez Almeida J., Kneer F.* Inter-network magnetic fields observed with sub-arcsec resolution // Astronomy and Astrophysics. V. 407. P. 741-757. 2003.
7. *Gingerich O., Noyes R.W., Kalkofen W., Cuny Y.* The Harvard-Smithsonian reference atmosphere // Solar Physics. V. 18(3) P. 347-365. 1971.
8. *Holweger H., Müller E.A.* The photospheric barium spectrum: solar abundance and collision broadening of Ba II lines by hydrogen // Solar Physics. V. 39. P. 19-30. 1974.
9. *Kosugi T., Matsuzaki K., Sakao T., et al.* The Hinode (Solar-B) Mission: An Overview // Solar Physics. V. 243(1). P. 3-17. 2007.
10. *Landi Degl'Innocenti, E.* MALIP – a programme to calculate the Stokes parameter of magnetoactive Fraunhofer lines // Astronomy and Astrophysics Supplement Series. V. 25. P. 379-390. 1976.
11. *Lites B.W., Akin D.L., Card G., et al.* The Hinode Spectro-Polarimeter // Solar Physics. V. 283. P. 579-599. 2013.
12. *Lites B.W., Kubo M., Socas-Navarro, H., et al.* The Horizontal Magnetic Flux of the Quiet-Sun Internetwork as Observed with the Hinode Spectro-Polarimeter // The Astrophysical Journal. V. 672. P. 1237-1253. 2008.
13. *Lites B.W., et al.* Are Internetwork Magnetic Fields in the Solar Photosphere Horizontal or Vertical? // The Astrophysical Journal, V. 835:14. 2017.
14. *Mathys G.* The diagnosis of stellar magnetic fields from spectral line profiles recorded in circularly polarized light // Astronomy and Astrophysics. V. 189. P. 179-193. 1988.
15. *Rees D.E. and Semel M.D.* Line formation in an unresolved magnetic element - A test of the centre of gravity method // Astronomy and Astrophysics. V. 74. P 1-5. 1979
16. *Semel M.* Contribution à létude des champs magnétiques dans les régions actives solaires // Annales d'Astrophysique. V. 30. P. 513-513. 1967.
17. *Stenflo J.O.* Magnetic-Field Structure of the Photospheric Network // Solar Physics. V. 32. P. 41-63. 1973.
18. *Stenflo J.O.* Horizontal or vertical magnetic fields on the quiet Sun. Angular distributions and their height variations // Astronomy and Astrophysics. V. 555. P. 132. 2013.
19. *Tsuneta S., Ichimoto, K., Katsukawa, Y., et al.* The Solar Optical Telescope for the Hinode Mission: An Overview // Solar Physics. V. 249. P. 167-196. 2008.

FIGURE CAPTIONS

Fig. 1. Top row - data from session 20070310_1137 (quiet photosphere). Bottom row - session 20141024_0031 (data taken for areas of penumbra). Diagrams (a,b,d,e) - comparison of the values of the longitudinal magnetic field fluxes f-$B_{||}$, obtained by the ME-inversion method and the COG method. Diagrams (c,f) - comparison of $B_{\text{IV,6301}}$ and $B_{\text{IV,6302}}$, values obtained by the COG method.

Fig. 2. Maps of the investigated sites. (a) - map of $\log_{10}(B_{\text{IV}})$ magnitude, black and white cutoff at levels 1 and 2.5 (10 and 310 Gs) for session 20070310_1137, B_{IV}denotes the longitudinal field flux measured by the COG method averaged over the two lines. (b) and (c) are the I_{C} brightness map and mask highlighting penumbra regions (I_{C}= [0.3 ... 0.8] $I_{(\text{QS})}$)) for session 20141024_0031, $I_{\text{QS}}$is the average brightness of the quiet Sun.

Fig. 3. Comparison of longitudinal field strength values. (a) and (b) comparison of the field obtained by calculation from synthetic Stokes profiles $B_{\text{I}\pm\text{V}}$ and the model field $B_{||} = B_0 \cdot \cos(\gamma)$ for the Fe I λ 6302 and 6301 Å lines. (c) Comparison of the calculated fields for the two lines with each other. On the *OX* axis is the logarithm of the field given in the model in Gauss. On the *OY* axis is the logarithm of the field ratio. The synthetic Stokes profiles were calculated using the HOLMU photospheric model [Holweger & Muller, 1974] for 7 values of the angle of inclination of the field vector to the line of sight and a set of field strength values.

Fig. 4. Calculation of response functions for the Fe I λ 6301 and 6302 Å lines using the one-dimensional HSRA [Gingerich et al., 1971] and HOLMU [Holweger & Muller, 1974] photospheric models. In a layer of width Δh = 10 km, a perturbation of the magnetic field strength B of magnitude 10 Gs was run over all heights of the photosphere, Stokes profiles were constructed, and from them the response of the magnitude $B_{\text{I}\pm\text{V}}$ was calculated .

Fig. 5. Comparison of effective occlusion heights for different segments of the spectral line profile.

Fig. 6. Model calculations of magnetic field reversal from vertical to horizontal direction. In the plots h_{t} (Height of Turn) is the average height of the turn, $\Delta h_{\text{t}}$is the extent of the turn, $|B_{\text{I}\pm\text{V}}|$ is the longitudinal field strength calculated from the model-calculated I and V Stokes profiles, B_0= the strength given in the model, $k_{12}$is the ratio of strengths $B_{\text{I}\pm\text{V}}$, calculated for Fe I λ 6301 and 6302 Å lines. Figure (a) - variation of $k_{12}$for a series of B_0values from 50 to 2500 Gs; the field was rotated by 90° over an altitude interval of 150 km at three positions of the center of rotation in height h_{t}. (b) and (c) calculation in which the field was unfolded at one point (Δh_{t}= 0), a series of $h_{(\text{t})}$ values was set and the dependence on the photospheric model was traced, as well as the variation of (b), the $k_{(12)}$ value at$_{\text{B}(0)}$= 900 Gs, and (c), the observed longitudinal field at B_0= 600, 900, and 1200 Gs.

Fig. 7. The central part of the 40×40" map of session 20070310_1137. (a) - magnetogram of B_{IV}, cutoff levels ± 300 Gs. (b) - map of $\log_{10}(k_{12})$ values, cutoff levels [0 ... 0.2] (k_{12} ~[1 ... 1.58]); the black mask covers regions without magnetic field for which $W_P < 3.3$ mÅ.

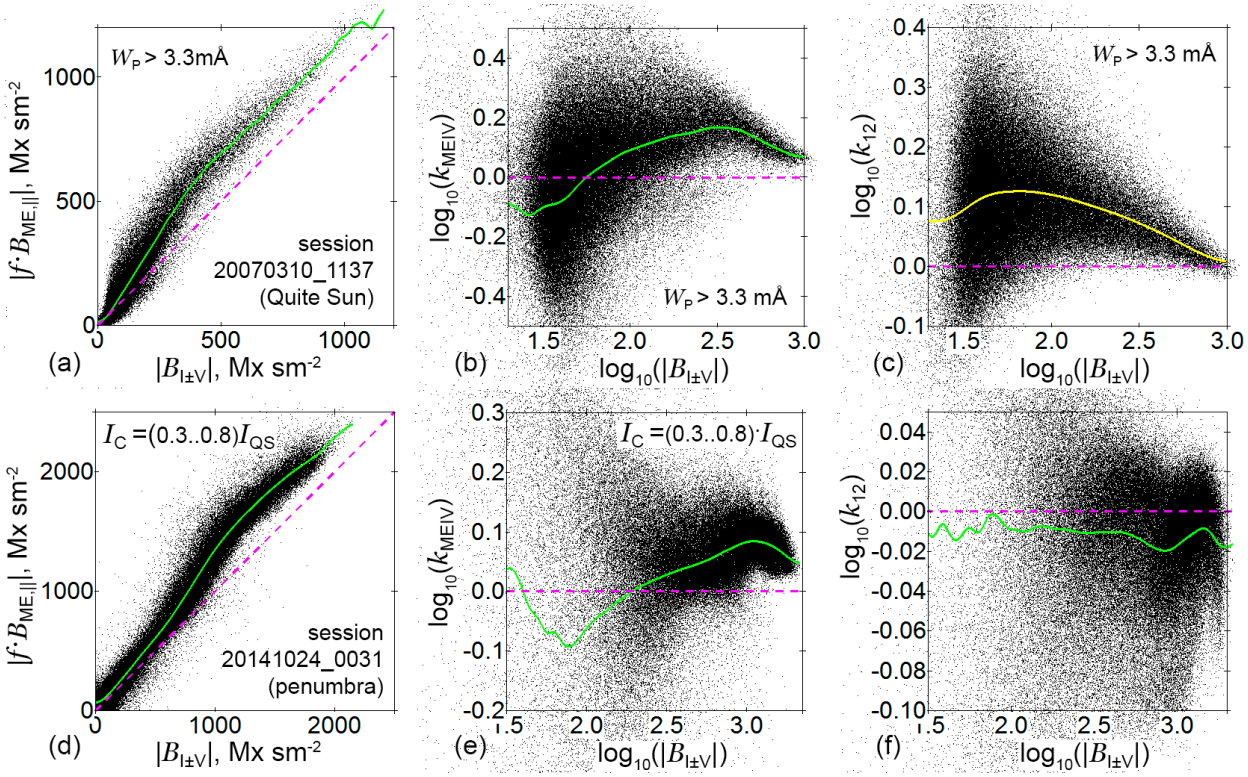
W_P > 3.3mÅ
session
20070310_1137
(Quite Sun)
(a)
$|f \cdot B_{ME,||}|$, Mx sm^{-2}
$|B_{l\pm V}|$, Mx sm^{-2}
(b)
$\log_{10}(k_{MEIV})$
$\log_{10}(|B_{l\pm V}|)$
W_P > 3.3 mÅ
(c)
$\log_{10}(k_{12})$
I_C =(0.3..0.8)I_{QS}
session
20141024_0031
(penumbra)
(d)
(e)
(f)

Fig. 1.

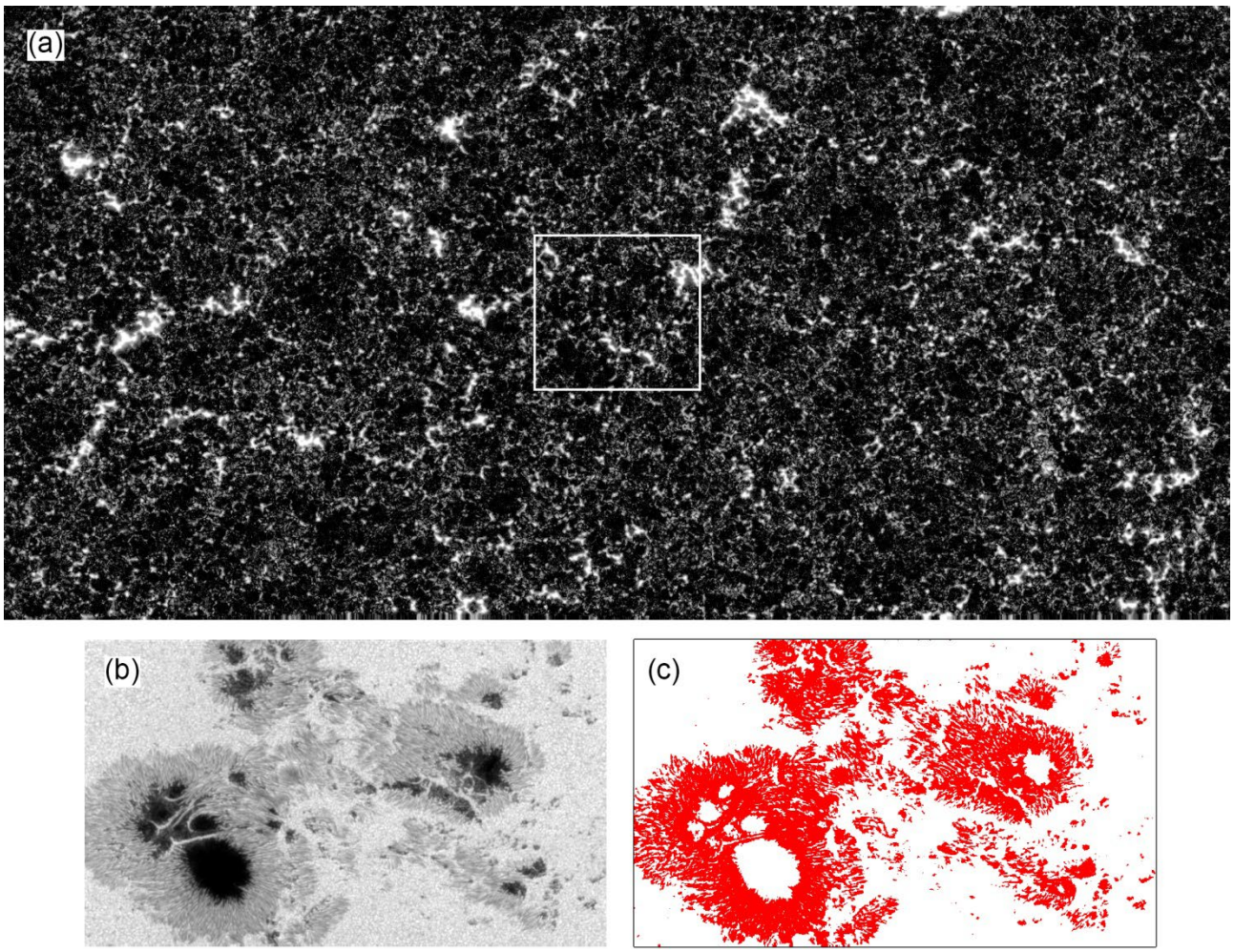
(a)
(b)
(c)

Fig. 2.

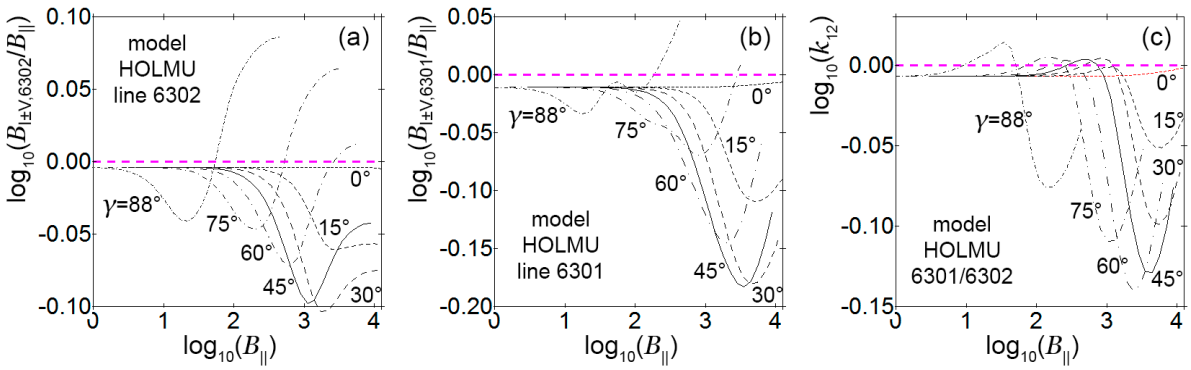
model
HOLMU
line 6302
(a)
γ=88°
75°
60°
45°
30°
15°
0°
model
HOLMU
line 6301
(b)
model
HOLMU
6301/6302
(c)
log10(B||)

Fig. 3.

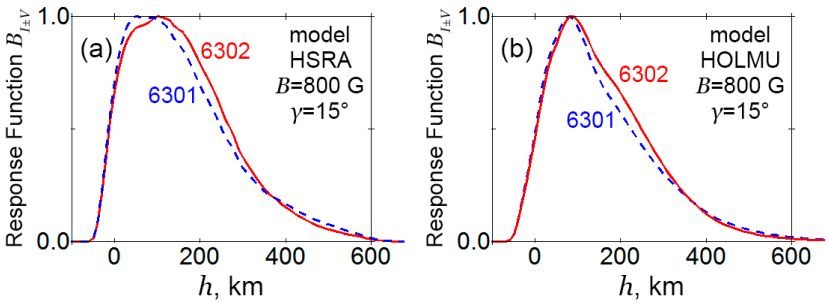

Fig. 4.

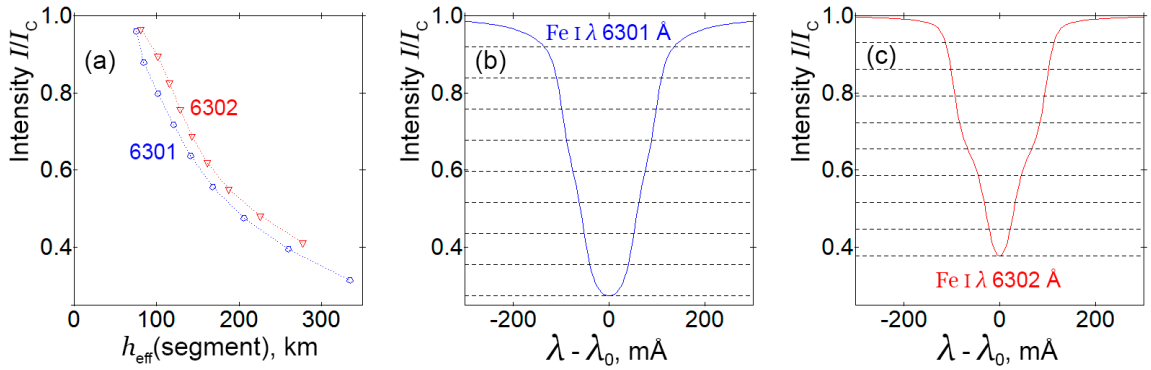

Fig. 5.

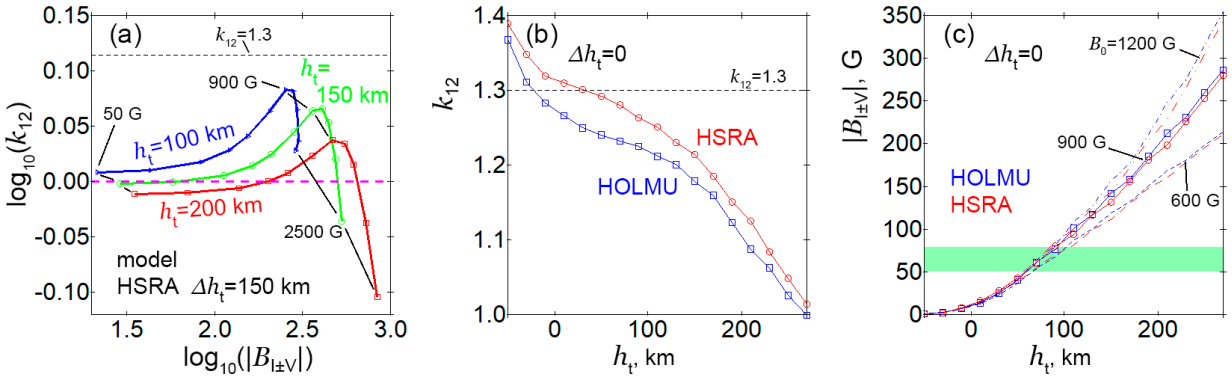

Fig. 6.

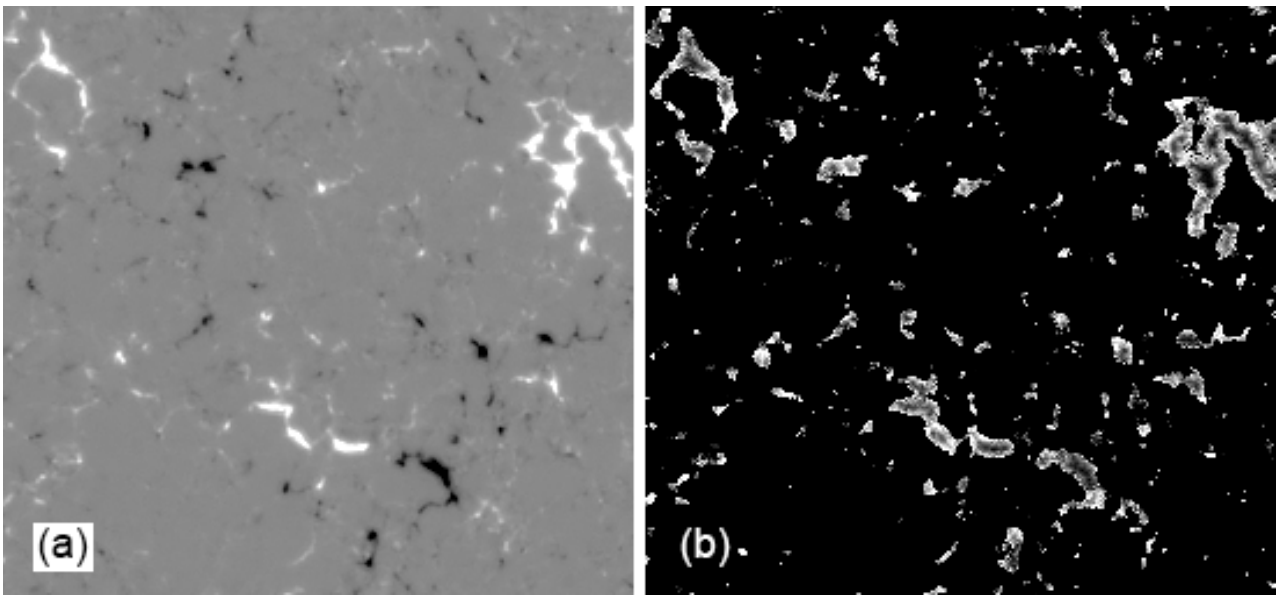

Fig. 7.